Computational Strategies for Simulation of Water Pollution Management

SONER AYDINLIK, AHMET KIRIS
Department of Mathematics, Faculty of Science and Letters
Istanbul Technical University
Istanbul
TURKEY

Abstract: This paper investigates a pollution model for a closed system consisting of three physically interconnected lakes. The pollutant source enters the first lake, while the exchange of contaminants among the lakes is described by a coupled system of first-order differential equations. To obtain accurate numerical solutions, the Smooth Composite Shifted Legendre Pseudospectral Method is applied. The contamination levels in each lake are examined under three pollutant loading scenarios: impulsive, exponentially decaying, and periodic inputs. The convergence and error of the method are analyzed. Numerical results and residual errors are compared with those obtained from established methods in the literature to assess the accuracy and stability of the scheme. The results demonstrate that the proposed approach yields reliable and efficient approximations, indicating that it can serve as a practical numerical tool for modeling pollutant transport in interconnected lake systems and supporting water quality assessment studies.

Key-Words: Water Pollution Management, Lake Contamination, Shifted Legendre Spectral Method, Numerical Simulation, Error Estimation, Residual Analysis.

Received: June 29, 2025. Revised: October 9, 2025. Accepted: November 15, 2025. Published: May 21, 2026.

Nomenclature

$u_i(t)$	Total pollutant in lake i
$p(t)$	Pollutant input rate
V_i	Volume of the lake i
F_{ij}	The rate of flow from the lake i to the lake j

1 Introduction

When the main way of moving water is by channels and quickly mixing inside each basin, interconnected lake systems are naturally shown as interacting compartments. In this setting, the system's state is effectively defined by the pollutant mass in each lake, with the coupling arising from inter-basin transfer rates. Compartmental formulations and their adaptations have been frequently employed in the literature to tackle lake contamination challenges, [1], [2], [3], [4], [5], [6], [7], [8], [9].

A frequent outcome of this methodology is a connected system of first-order initial value problems. Even if the structure is easy to work with because of the assumptions of constant volumes, uniform transfer rates, and well-mixed basins, the dynamics that follow could still be hard to calculate when the coupling is strong.In that case, the solution might be more sensitive to parameters, and standard time-marching solvers might have stability issues or take a long time to converge. To do this, you need to use high-precision discretizations that can handle coupled dynamics well.

This study examines a time-dependent contamination model for three interlinked lakes. People think of each lake as a basin with a constant volume V_i that is mixed evenly. At a rate of $p(t)$, an external input is added to the first lake. Let $u_i(t)$ be the amount of pollutants in lake i at time t. The concentration in the ith lake is given by

$$c_i(t) = \frac{u_i(t)}{V_i}, \quad i = 1,2,3. \tag{1}$$

Using mass conservation leads to a system of first-order differential equations in which each compartment changes based on the balance of incoming and outgoing fluxes.

We use the Smooth Composite Shifted Legendre Pseudospectral Method (SCSLPM) for the numerical work. Pseudospectral methods are well-known for providing high-order accuracy for solutions that are smooth enough with only a reasonable amount of computation, [10]. The composite construction enhances resilience by segmenting the time interval and ensuring continuity across subinterval interfaces, which is beneficial for coupled systems.

The remainder of the paper is organized as follows. After presenting the governing model and the considered input scenarios, we describe the SCSLPM discretization and analyze convergence and error behavior. The numerical section reports comparisons with reference solutions from the literature and includes additional tests illustrating the method's performance for nonlinear extensions of the classical model.

2 Mathematical Formulation

In this section, a mathematical model describing the pollution dynamics in an interconnected system of three lakes, as illustrated in Figure 1, is presented. The lakes are connected through channels that allow the transport of water and pollutants between them. It is assumed that each lake is perfectly mixed, so that the pollutant concentration is spatially uniform within each lake.

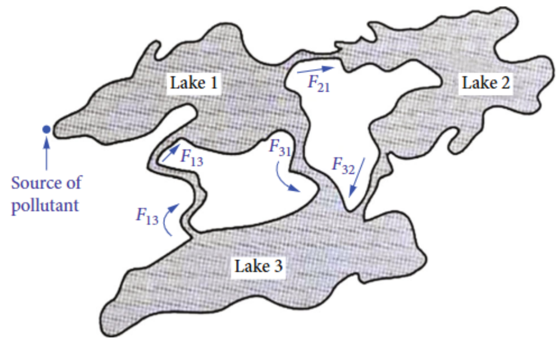

Fig. 1: Interconnected three-lake system, Source: [11].

Let $u_i(t)$ denote the amount of pollutant in lake i at time t, for $i = 1,2,3$. The volume of lake i is denoted by V_i, and F_{ij} represents the flow rate of water from lake i to lake j.

The pollution dynamics of the interconnected lake system are governed by the following system of first-order ordinary differential equations:

$$\begin{aligned}\frac{du_1(t)}{dt} &= \frac{F_{13}}{V_3}u_3(t) + p(t) - \frac{F_{31}}{V_1}u_1(t) - \frac{F_{21}}{V_1}u_1(t),\\ \frac{du_2(t)}{dt} &= \frac{F_{21}}{V_1}u_1(t) - \frac{F_{32}}{V_2}u_2(t),\\ \frac{du_3(t)}{dt} &= \frac{F_{31}}{V_1}u_1(t) + \frac{F_{32}}{V_2}u_2(t) - \frac{F_{13}}{V_3}u_3(t).\end{aligned} \tag{2}$$

where $p(t)$ refers to the external input by which pollution enters the first lake.

To ensure that the volume of each lake does not change with time, the inflow is taken to match the outflow. Under this condition, the following mass balance relations are obtained:

$$\begin{aligned}&\text{Lake 1:} \quad F_{13} = F_{21} + F_{31},\\ &\text{Lake 2:} \quad F_{21} = F_{32},\\ &\text{Lake 3:} \quad F_{31} + F_{32} = F_{13}.\end{aligned} \tag{3}$$

The system (2) is supplemented with the initial conditions

$$u_i(0) = u_{i,0}, \quad i = 1,2,3, \tag{4}$$

where $u_{i,0}$ denotes the initial pollutant mass contained in lake i.

The proposed formulation relies on one modeling structure to analyze pollution dynamics in interconnected lakes for impulsive, stepwise, and periodically varying contamination.

Impulse Input Model

The impulse input model represents an instantaneous release of pollutants into the lake system and is modeled using the Dirac delta function as

$$p(t) = p_0\,\delta(t - t_0), \tag{5}$$

where p_0 denotes the total amount of pollutant released at time t_0.

Step Input Model

The step input model describes a continuously increasing pollution source and is defined as

$$p(t) = \begin{cases} 0, & t < t_0,\\ \kappa t, & t \geq t_0, \end{cases} \tag{6}$$

where κ is a positive constant. In the numerical simulations, $\kappa = 100$ is selected.

Sinusoidal Input Model

The sinusoidal input model is employed to describe periodic pollutant sources and is given by

$$p(t) = \phi\left(1 + a\sin\left(\frac{2\pi t}{T}\right)\right), \tag{7}$$

where a is the normalized amplitude satisfying $0 \leq a \leq 1$, T denotes the period of oscillation, and ϕ represents the average pollutant input concentration.

3 Shifted Legendre smooth composite pseudo spectral method

In the context of solving initial or boundary value problems (IVP or BVP), one typically writes the approximation polynomial as,

$$y(x) = \sum_{n=0}^{N} a_n\,\varphi_n(x), \tag{8}$$

where

$$a_n = \frac{1}{\|\varphi_n\|^2}\sum_{j=0}^{N}\varphi_n(x_j)\,y(x_j)\,w_j. \tag{9}$$

In the above equation, N is polynomial degree, $\varphi_n(x)$ is an orthogonal polynomial and w_j is the Gauss Lobatto quadrature (GLQ) weight. In this study, shifted Legendre polynomials are used as trial functions in the pseudo spectral method. The first kind of shifted Legendre polynomials are introduced as

$$P_n^*(x) = \sum_{k=0}^{n}\frac{(-1)^{n+k}(n+k)!}{(n-k)!(k!)^2}(2x-1)^k, \tag{10}$$

respectively. The composite pseudo spectral methods are based on splitting the domain into the $M-$subdomains with the step size $h=\frac{(b-a)}{M}$. The collocation points are chosen as

$$x_k=\frac{x_k+1}{2},\quad (1-{x_k}^2)P_N'(x_k)=0,\quad k=0,1,\ldots,N. \tag{11}$$

The transformation to the j^{th} subdomain $\left[a+\frac{j(b-a)}{M},\ a+\frac{(j+1)(b-a)}{M}\right]$ is given as

$$t_{ki}=\frac{(b-a)}{M}\ (x_{Lk}+i)\,,\quad i=0,...,M-1. \tag{12}$$

The numerical solutions for the i^{th} subdomain are defined as

$$y_i(x)=\sum_{n=0}^{N}a_{in}P_n^*(x) \tag{13}$$

where

$$a_{in}=\alpha_n\sum_{j=0}^{N}\frac{1}{\left(P_N^*(x_j)\right)^2}y_i(x_j)\,P_n^*(x_j), \tag{14}$$

here

$$\alpha_n=\begin{cases}\frac{2n+1}{N(N+1)}, & n=0,1,...,N-1,\\ \frac{1}{(N+1)}, & n=N.\end{cases} \tag{15}$$

The m^{th} order derivatives of the approximation polynomials at the nodes are

$$y_i^{(m)}(x_k)=\sum_{j=0}^{N}d_{k,j}^{(m)}\,y_i(x_j). \tag{16}$$

where

$$d_{k,j}^{(m)}=\ \frac{1}{\left(P_N^*(x_j)\right)^2}\ \sum_{n=0}^{N}\alpha_nP_n^*(x_j)\,P_n^{*(m)}(x_k). \tag{17}$$

The expansion of (17) for Legendre is defined by [12], as

$$d_{k,j}^{(m)}=\frac{1}{\left(P_N^*(x_j)\right)^2}\sum_{n=0}^{N}\sum_{s=0}^{n}(-1)^{n+s}\frac{(x_i)^{s-m}(n+s)!}{\Gamma(s-m+1)(n-s)!\,s!}\times\alpha_nP_n^*(x_j)\,P_n^{*(m)}(x_k). \tag{18}$$

For the smoothness,

$$y_{i+1}^{(r)}(x_0)=y_i^{(r)}(x_N).\quad r=0,1,...,\lfloor m-1\rfloor \tag{19}$$

must be satisfied. The present methods reduce the problem to a set of algebraic equations. Combining the approximation polynomials for each subdomain, $y_i(x)$ yields the general solution, $P_N(x)\in C^{\lfloor m-1\rfloor}[a,b]$.

4 Convergence and error analyzes of Legendre SCPSM

4.1 Convergence analysis

Theorem 1. *Let $y_i(x)$ is a continuous function on $[0,1]$ and $\left|y_i^{(m)}(x)\right|\le C_i$. Then, the second equation of (14) converges uniformly to the function $y_i(x)$, when $N\to\infty$, [12]. Thus, $y(x)=\bigcup_{i=1}^{M}y_i(x)$ also converges.*

Proof. By using the orthogonality property of the shifted Legendre polynomials, a_{in} can be expressed as

$$a_{in}=(2n+1)\int_0^1 y_i(x)P_n^*(x)dx. \tag{20}$$

By using integration by parts and recursion relation of Legendre polynomials

$$a_{in}=\frac{1}{2}\int_0^1 {y_i}'(x)\sigma_1(x)\,dx,\quad n\ge 1, \tag{21}$$

where $\sigma_1(x)=P_{n-1}^*(x)-P_{n+1}^*(x)\le \mathrm{O}(n^0)$ and the same procedure is applied for one more time:

$$a_{in}=\frac{1}{2}\int_0^1 {y_i}''(x)\sigma_2(x)\,dx, \tag{22}$$

where $\sigma_2(x)=\frac{P_{n+2}^*(x)-P_n^*(x)}{4n+6}-\frac{P_n^*(x)-P_{n-2}^*(x)}{4n-2}\le \mathrm{O}(n^{-1})$. Performing the above procedures $(m-2)$ times gives

$$|a_{in}|\le \mathrm{O}\left(\frac{1}{n^{m-1}}\right). \tag{23}$$

Similar procedure to the one in the Chebyshev method gives an upper bound for the approximation

$$|y_i(x)|=\left|\sum_{n=0}^{\infty}a_{in}P_n^*(x)\right|\le\sum_{n=0}^{\infty}|a_{in}|\le|a_{i0}|+\sum_{n=1}^{\infty}|a_{in}|<\infty, \tag{24}$$

Consequently, the solution is bounded by

$$|y(x)|\le\max_{1\le i\le M}|y_i(x)|\le\max_{1\le i\le M}\left(|a_{i0}|+\sum_{n=1}^{\infty}|a_{in}|\right)<\infty. \tag{25}$$

□

4.2 Error analysis

Theorem 2. *Assume that the approximation polynomial for i^{th} subinterval is defined by $P_N\,y_i=\sum_{n=0}^{N}a_{in}P_n^*(x)$. The error is presented as*

$$\|y_i-P_N\,y_i\|\le \mathrm{O}(\frac{1}{N^{m-2}}) \tag{26}$$

for $\forall\,y_i(x)\in H_w^m[0,1]$, $m\ge 0$, [12].

Proof. Since

$$\|y_i - P_N\, y_i\| \le \left| \sum_{n=N+1}^{\infty} a_n P_n^*(x) \right| \le \left| \sum_{n=N+1}^{\infty} a_n \right|, \tag{27}$$

then considering (27) with the integral test for series, we obtain

$$\|y_i - P_N\, y_i\| = \int_{N+1}^{\infty} a(x)dx \le \mathrm{O}\left(\frac{1}{N^{m-2}}\right). \tag{28}$$

□

5 Numerical illustrations

This section presents three test scenarios designed to assess the performance and accuracy of the proposed numerical method for the interconnected three-lake pollution model. Three representative pollutant input models—impulsive, step, and sinusoidal—are employed to investigate the system behavior. All approximate solutions are computed using *Mathematica*. For the numerical experiments, the polynomial degree is chosen as $N = 8$, and the number of subintervals is taken as $M = 4$. The accuracy of the method is evaluated by analyzing the corresponding residual errors.

$$\begin{aligned}
R_1(t) &= \left| \frac{du_1(t)}{dt} - \frac{F_{13}}{V_3}u_3(t) - p(t) + \frac{F_{31}}{V_1}u_1(t) + \frac{F_{21}}{V_1}u_1(t) \right|, \\
R_2(t) &= \left| \frac{du_2(t)}{dt} - \frac{F_{21}}{V_1}u_1(t) + \frac{F_{32}}{V_2}u_2(t) \right|, \\
R_3(t) &= \left| \frac{du_3(t)}{dt} - \frac{F_{31}}{V_1}u_1(t) - \frac{F_{32}}{V_2}u_2(t) + \frac{F_{13}}{V_3}u_3(t) \right|.
\end{aligned} \tag{29}$$

The physical parameters used in the simulations are adopted from, [3], and are given as

$$\begin{aligned}
&V_1 = 2900 \text{ mi}^3, \quad V_2 = 850 \text{ mi}^3, \quad V_3 = 1180 \text{ mi}^3, \\
&F_{13} = 38 \text{ mi}^3/\text{year}, \quad F_{21} = 18 \text{ mi}^3/\text{year}, \\
&F_{31} = 20 \text{ mi}^3/\text{year}, \quad F_{32} = 18 \text{ mi}^3/\text{year}, \\
&u_1(0) = 0, \quad u_2(0) = 0, \quad u_3(0) = 0.
\end{aligned} \tag{30}$$

5.1 Impulse input

In this subsection, the pollution dynamics of the interconnected three-lake system are investigated under an impulsively imposed pollutant input. An impulse input represents a sudden, one-time release of pollutants into a Lake, after which no additional contamination enters the system. Physically, this scenario corresponds to the instantaneous discharge of a finite amount of pollutant, such as the accidental release of a single barrel of chemicals at the initial time.

Mathematically, the impulsive pollutant source is modeled by a constant input function $p(t) = 100$, which is commonly adopted in the literature for comparison purposes, [3]. The numerical results obtained by the proposed method are compared with those from the Adomian decomposition method reported in [3], as presented in Table 1 (Appendix), where excellent agreement between the two approaches is observed.

The time evolution of the pollutant contents $u_1(t)$, $u_2(t)$, and $u_3(t)$ for the impulse input case is shown in Figure 2.

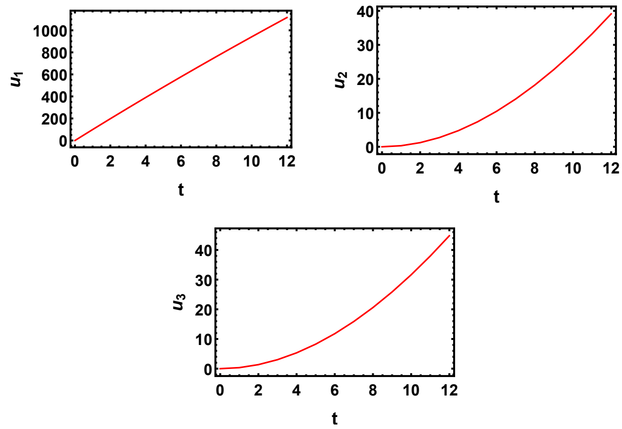

Fig. 2: Time evolution of $u_1(t)$, $u_2(t)$, and $u_3(t)$ for the impulse input. Source: created by the authors.

5.2 Step input

In this subsection, the pollution dynamics of the interconnected three-lake system are investigated under a stepwise increasing pollutant input. A step input represents a continuous and steady introduction of pollutants into a lake at a constant rate, starting from time zero.This situation can be interpreted as a case in which an industrial facility begins operating at the initial time and continuously releases untreated wastewater into the lake, while the aquatic system is assumed to be uncontaminated at the beginning of the process.

For the numerical simulations, the external pollutant input is taken as $p(t) = 100t$. This function represents a pollution source whose strength increases progressively over time. The discharge begins at $t = 0$ and grows linearly throughout the computational time interval.

Results obtained with the proposed method are compared with those reported for the Adomian decomposition method in [3], as summarized in Table 1. The table lists the pollutant concentrations in the three lakes, represented by $u_1(t)$, $u_2(t)$, and $u_3(t)$, computed by both approaches. The two sets of results remain very close to each other, indicating that the proposed numerical scheme reproduces the system dynamics with high accuracy under a stepwise increasing pollutant input. Figure 3 illustrates the time evolution of $u_1(t)$, $u_2(t)$, and $u_3(t)$ under the step input scenario.

Table 1: Results for step input model.

n	t_i	Adomian method, [3]			Proposed method		
		$u_1(t_i)$	$u_2(t_i)$	$u_3(t_i)$	$u_1(t_i)$	$u_2(t_i)$	$u_3(t_i)$
0	0.00	0.00000	0.00000	0.00000	0.00000	0.00000	0.00000
1	0.01	0.00500	1.03440E-07	1.14940E-07	0.00500	1.03440E-07	1.14940E-07
2	0.02	0.02000	8.27444E-07	9.19420E-07	0.02000	8.27444E-07	9.19420E-07
3	0.03	0.04499	2.79239E-06	3.10284E-06	0.04500	2.79239E-06	3.10284E-06
4	0.04	0.07999	6.61842E-06	7.35439E-06	0.07999	6.61842E-06	7.35439E-06
5	0.05	0.12497	1.29255E-05	1.43631E-05	0.12497	1.29255E-05	1.43631E-05
6	0.06	0.17995	2.23333E-05	2.48178E-05	0.17995	2.23333E-05	2.48178E-05
7	0.07	0.24493	3.54615E-05	3.94072E-05	0.24493	3.54615E-05	3.94072E-05
8	0.08	0.31989	5.29292E-05	5.88197E-05	0.31989	5.29292E-05	5.88197E-05
9	0.09	0.40484	7.53557E-05	8.37436E-05	0.40484	7.53557E-05	8.37436E-05
10	0.10	0.49978	1.03360E-04	1.14867E-04	0.49978	1.03360E-04	1.14867E-04

Source: created by the authors

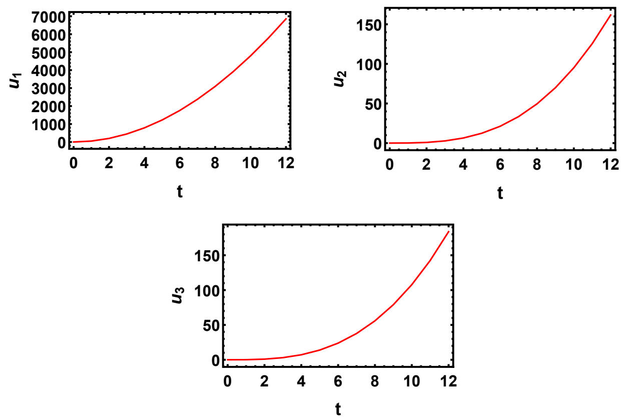

Fig. 3: Time evolution of $u_1(t)$, $u_2(t)$, and $u_3(t)$ for the step input. Source: created by the authors.

5.3 Sinusoidal input

In this subsection, the pollution dynamics of the interconnected three-lake system are investigated under a sinusoidal pollutant input, which represents a periodic discharge of pollutants into the lakes. Many industrial waste sources operate predominantly during daylight hours, resulting in higher pollutant production during the day compared to nighttime. Consequently, the pollutant levels can be modeled using a periodic function of the form $p(t) = 1 + \sin(t)$.

This sinusoidal input scenario corresponds to a situation where the pollutant enters the system with an average concentration and then varies periodically around that average. The numerical results obtained by the proposed method are compared with those from the Adomian decomposition method reported in [3], as presented in Table 2. The comparison highlights the accuracy of the proposed method in capturing the periodic behavior of the pollutant concentrations $u_1(t)$, $u_2(t)$, and $u_3(t)$ in the lakes.

In Table 3, Table 4 and Table 5, the errors of BPM, [4], BCM, [5], and GWM, [13], are reported for $N = 10$, while the proposed method uses $N = 8$ and $M = 4$. The computational CPU times of the methods are given in Table 6. To examine the accuracy and convergence properties of the proposed method, absolute residual errors associated with the governing equations are computed for several values of N and M. The resulting error distributions are presented in Figure 1 (Appendix). As the polynomial degree and the number of subintervals increase, the magnitude of the residual errors decreases noticeably, indicating improved numerical accuracy and stable convergence of the method. Figure 4 illustrates the temporal variation of the pollutant contents $u_1(t)$, $u_2(t)$, and $u_3(t)$ under sinusoidal pollutant input.

Table 2: Results for sinusoidal input model with updated decimal formatting and high-precision values.

n	t_i	Adomian method, [3]			Proposed method (SCSLPM)		
		$u_1(t_i)$	$u_2(t_i)$	$u_3(t_i)$	$u_1(t_i)$	$u_2(t_i)$	$u_3(t_i)$
0	0.00	0.00000	0.00000	0.00000	0.00000	0.00000	0.00000
1	0.01	0.01005	3.11344E-07	3.45950E-07	0.01005	3.11344E-07	3.45947E-07
2	0.02	0.02020	1.24937E-06	1.38826E-06	0.02020	1.24937E-06	1.38826E-06
3	0.03	0.03044	2.82007E-06	3.13366E-06	0.03044	2.82007E-06	3.13366E-06
4	0.04	0.04079	5.02943E-06	5.58885E-06	0.04079	5.02943E-06	5.58885E-06
5	0.05	0.05123	7.88343E-06	8.76053E-06	0.05123	7.88343E-06	8.76053E-06
6	0.06	0.06178	0.00001	0.00001	0.06178	0.0000113881	0.0000126554
7	0.07	0.07242	0.00002	0.00002	0.07242	0.0000155493	0.0000172802
8	0.08	0.08316	0.00002	0.00002	0.08316	0.0000203730	0.0000226415
9	0.09	0.09399	0.00002	0.00003	0.09399	0.0000258653	0.0000287461
10	0.10	0.10493	0.00003	0.00004	0.10493	0.0000320321	0.0000356007

Source: created by the authors

Table 3: Comparison of residual errors $R_1(t)$

t	BPM, [4]	BCM, [5]	GWM, [13]	Present Method
0.2	1.26760×10^{-13}	1.24480×10^{-13}	1.15200×10^{-13}	1.28481×10^{-13}
0.4	1.21070×10^{-13}	2.53460×10^{-13}	4.38538×10^{-15}	1.08247×10^{-14}
0.6	9.85880×10^{-14}	3.91240×10^{-13}	5.55112×10^{-17}	5.88418×10^{-15}
0.8	5.07370×10^{-14}	5.41460×10^{-13}	1.13243×10^{-14}	8.88178×10^{-16}
1.0	4.89280×10^{-11}	4.96510×10^{-11}	2.08822×10^{-12}	5.21805×10^{-15}

Source: created by the authors

Table 4: Comparison of residual errors $R_2(t)$

t	BPM, [4]	BCM, [5]	GWM, [13]	Present Method
0.2	6.61150×10^{-16}	1.76210×10^{-15}	1.49896×10^{-15}	6.17679×10^{-16}
0.4	8.09190×10^{-16}	3.45760×10^{-15}	5.23647×10^{-17}	4.59702×10^{-17}
0.6	9.37060×10^{-16}	5.08630×10^{-15}	1.90972×10^{-18}	9.54098×10^{-18}
0.8	1.01970×10^{-15}	6.64640×10^{-15}	1.37462×10^{-16}	1.30104×10^{-17}
1.0	5.45960×10^{-13}	5.38930×10^{-13}	2.35596×10^{-14}	6.15827×10^{-17}

Source: created by the authors

Table 5: Comparison of residual errors $R_3(t)$

t	BPM, [4]	BCM, [5]	GWM, [13]	Present Method
0.2	7.45460×10^{-16}	1.52350×10^{-15}	1.67600×10^{-15}	8.62972×10^{-16}
0.4	9.14160×10^{-16}	2.95500×10^{-15}	6.12146×10^{-17}	3.96818×10^{-17}
0.6	1.06390×10^{-15}	4.28400×10^{-15}	1.07865×10^{-18}	2.60209×10^{-18}
0.8	1.16670×10^{-15}	5.51610×10^{-15}	1.54378×10^{-16}	1.21431×10^{-17}
1.0	6.09290×10^{-13}	6.17950×10^{-13}	2.63161×10^{-14}	5.03070×10^{-17}

Source: created by the authors

Table 6: Comparison of CPU times

Method	CPU time (s)
GWM, [13]	0.080411
RK4 ($\Delta t = 0.1$)	0.011045
Mathematica default solver	0.104975
Present method	0.067534

Source: created by the authors

5.4 Nonlinear extension of the model

In many natural aquatic environments, pollutant removal does not follow a strictly linear pattern. Mechanisms such as flocculation, sedimentation, and chemical transformations often become more pronounced as contaminant lev-

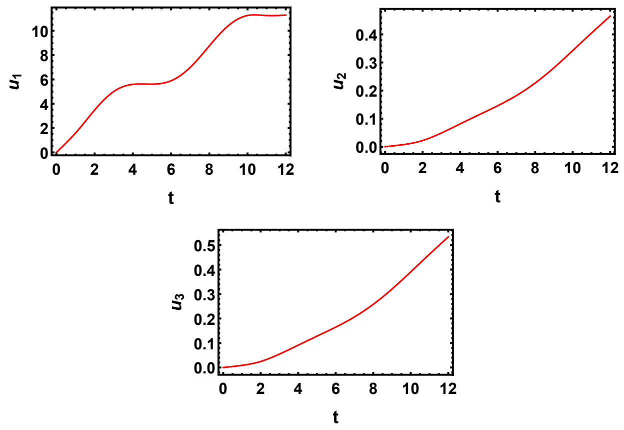

Fig.4: Time evolution of $u_1(t)$, $u_2(t)$, and $u_3(t)$ for the sinusoidal input. Source: created by the authors.

els increase. To capture this concentrationdependent behavior, environmental models commonly incorporate nonlinear loss terms.

In order to assess the behavior of the proposed numerical scheme in a nonlinear setting, the classical lake pollution model is extended by adding a quadratic removal term in the first lake. This modification reflects the fact that attenuation mechanisms are typically more active near the pollution source, where contaminant concentrations are generally higher than in the downstream lakes.

With this modification, the governing system takes the form

$$\frac{du_1(t)}{dt} = \frac{F_{13}}{V_3}u_3(t) + p(t) - \frac{F_{31}}{V_1}u_1(t) - \frac{F_{21}}{V_1}u_1(t) - k\,u_1(t)^2, \tag{31}$$

$$\frac{du_2(t)}{dt} = \frac{F_{21}}{V_1}u_1(t) - \frac{F_{32}}{V_2}u_2(t), \tag{32}$$

$$\frac{du_3(t)}{dt} = \frac{F_{31}}{V_1}u_1(t) + \frac{F_{32}}{V_2}u_2(t) - \frac{F_{13}}{V_3}u_3(t), \tag{33}$$

The coefficient k represents the nonlinear removal effect in the model. In particular, the quadratic term ku_1^2 describes the attenuation mechanism associated with concentration-dependent processes such as particle aggregation or settling. In the numerical experiments considered here, the external pollutant input is taken to be sinusoidal.

Figure 5 illustrates the temporal evolution of $u_1(t)$ for several values of the parameter k. The results show that the strength of the removal mechanism has a noticeable influence on the system behavior. As k increases, the peak pollutant concentration in the first lake decreases significantly, indicating a stronger attenuation effect.

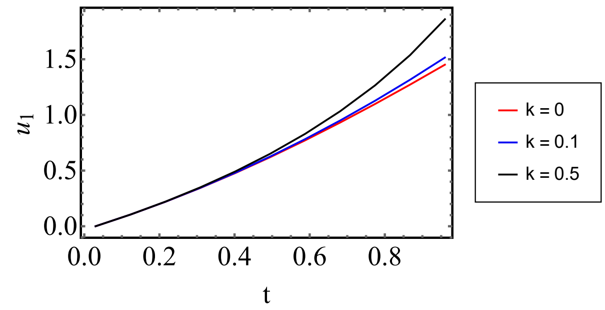

Fig. 5: Temporal evolution of $u\ (t)$ under sinusoidal pollutant input. Source: created by the authors.

Nonlinear test cases are also investigated in order to evaluate the performance of the SCSLPM beyond linear model. The results show that the approach stays accurate even when the system dynamics get more complicated. In these contexts, the system reliably generates precise approximations, indicating that the suggested approach is applicable to both fundamental configurations and complex pollution dynamics.

6 Conclusions

A pollution model is studied for a system of three interconnected lakes. The model illustrates the transfer of pollution between lakes through a series of first-order differential equations influenced by a time-dependent input $p(t)$ that enters the initial lake. To generate numerical approximations, the Smooth Composite Shifted Legendre Pseudospectral Method (SCSLPM) are used.

Three different cases are analyzed within a unified modeling framework: impulsive release, sequentially rising input, and sinusoidal forcing. The time histories of $u_1(t)$, $u_2(t)$, and $u_3(t)$ for each example aligned with the outcomes obtained by the Adomian Decomposition Method. Residual-based error measurements, alongside convergence analysis, demonstrate that the suggested methodology yields consistent and precise approximations for the evaluated benchmarks, while ensuring a reasonable computational expense.

These results validate the efficacy of SCSLPM as a numerical instrument for lake pollution models incorporating coupled dynamics and time-dependent inputs, and they underscore the use of compartment-based formulations in examining contaminant dispersion across interconnected lake networks.

References

[1] J. Biazar, M. Shahbala, H. Ebrahimi, VIM for solving the pollution problem of a system of lakes, Discrete Dynamics in Nature and Society 2010 (2010) 829152. https://doi.org/10.1155/2010/829152

[2] J.C. Varekamp, Lake contamination models for evolution towards steady state, *Jour-*

nal of Limnology **62**(1) (2003) 67–72. https://doi.org/10.4081/jlimnol.2003.s1.67

[3] J. Biazar, L. Farrokhi, M.R. Islam, Modeling the pollution of a system of lakes, *Applied Mathematics and Computation* **178**(2) (2006) 423–430. https://doi.org/10.1016/j.amc.2005.11.056

[4] S. Yüzba, G. Yldrm, Boubaker collocation method for approximate solutions of the model of pollution for a system of lakes, *Turkish Journal of Mathematics and Computer Science* **16**(1) (2024) 240–254. https://doi.org/10.47000/tjmcs.1167568

[5] S. Yüzba, N. ahin, M. Sezer, A collocation approach to solving the model of pollution for a system of lakes, *Mathematical and Computer Modelling* **55**(3–4) (2012) 330–341. https://doi.org/10.1016/j.mcm.2011.08.007

[6] B. Benhammouda, H. Vázquez-Leal, L. Hernández-Martínez, Modified differential transform method for solving the model of pollution for a system of lakes, *Discrete Dynamics in Nature and Society* **2014**(645726) (2014) 1–7. https://doi.org/10.1155/2014/645726

[7] V.F. Hatipolu, A novel model for the contamination of a system of three artificial lakes, *Discrete and Continuous Dynamical Systems - Series S* **14**(7) (2021) 2261–2272. https://doi.org/10.3934/dcdss.2020176

[8] N. Yönet, B. Gürbüz, A. Gökçe, An alternative numerical approach for an improved ecological model of interconnected lakes with a fixed pollutant, *Computational and Applied Mathematics* **42** (2023) 56. https://doi.org/10.1007/s40314-023-02191-3

[9] M. Adel, M.M. Khader, Pollution dynamics in an interconnected lake system: modeling and simulation using the finite element method, *Journal of Applied Mathematics and Computational Mechanics* **24**(1) (2025) 5–17. https://doi.org/10.17512/jamcm.2025.1.01

[10] S. Aydinlik, An efficient method for oxygen diffusion in a spherical cell with nonlinear oxygen uptake kinetics, *International Journal of Biomathematics* **15**(5) (2022) 2250019. https://doi.org/10.1142/S179352452250019X

[11] F.R. Giordano, M.D. Weir, *Differential Equations: A Modern Approach*, Addison–Wesley Publishing Company, Boston, USA (1991). ISBN: 978-0486619415. `https://books.google.com.tr/books/about/Differential_Equations.html?id=gNspAQAAMAAJ&redir_esc=y` [Access Date: 01/01/2026]

[12] M. Abdelhakem, D. Abdelhamied, M.G. Alshehri, M. El-Kady, Shifted Legendre fractional pseudospectral differentiation matrices, *Fractals* **29**(1) (2021) 2240038. https://doi.org/10.1142/s0218348x22400382

[13] S. Gümgüm, A fast and reliable numerical approach for solving lake pollution problem, *Balkesir Üniversitesi Fen Bilimleri Enstitüsü Dergisi* **27**(2) (2025) 736–749. https://doi.org/10.25092/baunfbed.1676679

Contribution of individual authors to the creation of a scientific article (ghostwriting policy)

Soner Aydinlik developed the methodology, carried out the numerical simulations, analyzed the results, and prepared the original manuscript draft. Ahmet Kiris contributed to the conceptual design of the study, supervised the research process, reviewed the mathematical formulation, and revised the manuscript critically.

The authors equally contributed to the final interpretation of the results, the discussion, and the approval of the final version of the manuscript.

Sources of funding for research presented in a scientific article or scientific article itself

Funding for this research was provided by Istanbul Technical University (Project No. TGA-2025-46490).

Conflict of Interest

The authors have no conflicts of interest to declare that are relevant to the content of this article.

Creative Commons Attribution License 4.0 (Attribution 4.0 International, CC BY 4.0)

APPENDIX

Table 1: Results for impulse input model.

n	t_i	Adomian method, [3]			Proposed method		
		$u_1(t_i)$	$u_2(t_i)$	$u_3(t_i)$	$u_1(t_i)$	$u_2(t_i)$	$u_3(t_i)$
0	0.00	0.00000	0.00000	0.00000	0.00000	0.00000	0.00000
1	0.01	0.99993	0.00003	0.00003	0.99993	0.00003	0.00003
2	0.02	1.99974	0.00012	0.00014	1.99974	0.00012	0.00014
3	0.03	2.99941	0.00028	0.00031	2.99941	0.00028	0.00031
4	0.04	3.99900	0.00049	0.00055	3.99895	0.00050	0.00055
5	0.05	4.99895	0.00076	0.00086	4.99836	0.00078	0.00086
6	0.06	5.99836	0.00112	0.00124	5.99764	0.00112	0.00124
7	0.07	6.99764	0.00152	0.00169	6.99679	0.00152	0.00169
8	0.08	7.99679	0.00198	0.00221	7.99581	0.00198	0.00221
9	0.09	8.99581	0.00251	0.00279	8.99470	0.00251	0.00279
10	0.10	9.99345	0.00310	0.00345	9.99345	0.00310	0.00345

Source: created by the authors

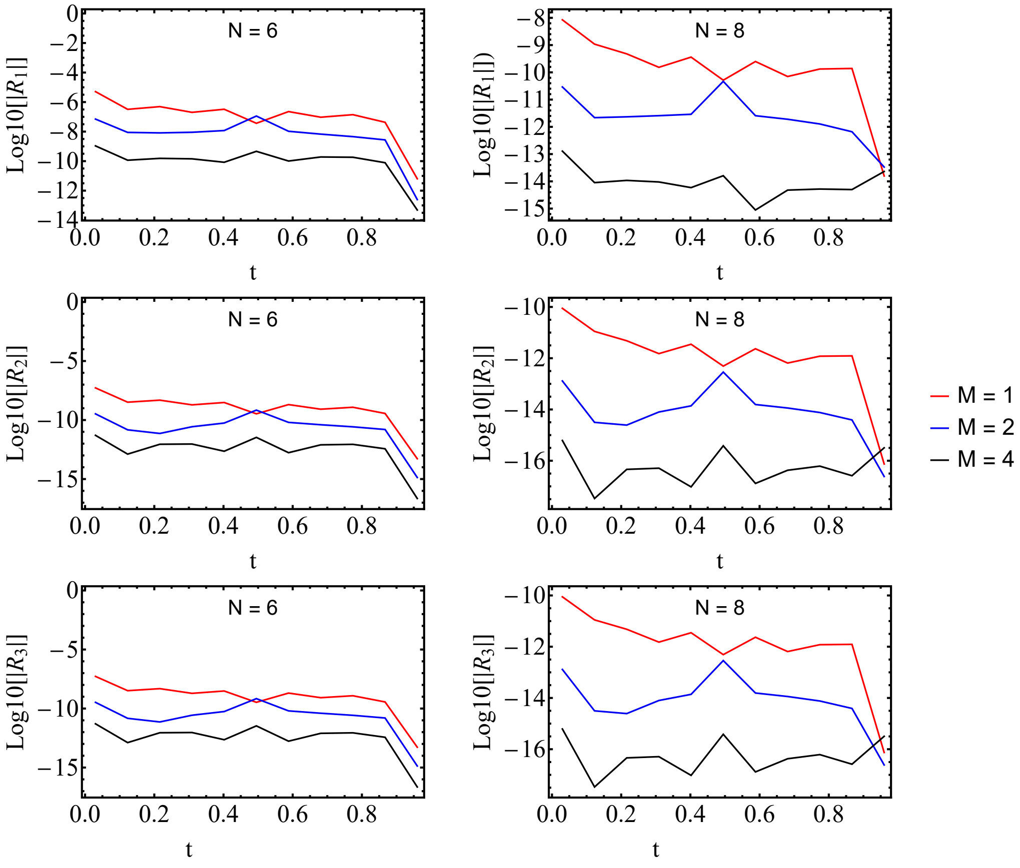

Fig. 1: Logarithmic plots of the residual functions R_1, R_2 and R_3 for different values of N and M. Source: created by the authors.